Indian Journal of Chemical Technology
Vol. 30, March 2023, pp. 151-164
DOI: 10.56042/ijct.v30i2.64532

Cereal based traditional beverage of tella residue (attela) as a green organic pollutant sorbent for methylene blue dye removal: Equilibrium, kinetics and thermodynamic studies

Gietu Yirga Abate*[1], Duong Tuan Anh Nguyen[2], Adugna Nigatu Alene[3], Desalegn Adisu Kassie[3], Yetayesh Abebaw Addiss[4] & Smegnew Moges Mintesinot[5]

[1]Department of Chemistry, College of Natural and Computational Science, Injibara University, Injibara, Ethiopia

[2]Department of Chemical Engineering, College of Engineering, National Taiwan University of Science and Technology, Taipei, Taiwan

[3]Department of Chemical Engineering, Faculty of Chemical and Food Engineering, Bahir Dar University Institute of Technology, Bahir Dar University, Bahir Dar, Ethiopia

[4]Department of Chemistry, Faculty of Natural and Computational Science,Woldia University, Woldia, Ethiopia

[5]Department of Mechanical Engineering, Faculty of Mechanical and Industrial Engineering, Bahir Dar Institute of Technology-Bahir Dar University, BahirDar, Ethiopia

E-mail:geitu03@gmail.com

Received 15 July 2022; accepted 21 January 2023

Dyes are one the foremost hazardous pollutants that affects bio life including the flora and fauna and removing of those pollutants from contaminated environment are remarkable activities within the scientific community. In this respect, the current study is focused on preparation of physiochemical activated cereals based tella residue bio adsorbent for basic blue dye (MB) removal from aqueous environment. Different analytical methods have been utilized to assess the thermal stability, surface area, surface morphology, pore size, pore volume, surface functional group, and a few proximate analyses of the prepared bio adsorbents. The SEM and BET results of the adsorbents reveals physiochemical activation process assists for the formation of visible pores, cracks, irregular shape, and better surface area (51.32 m^2/g for RTR and 565m^2/g for ATR) respectively. The removal efficiencies of MB by RTR and ATR in an exceedingly batch experiment were 88.4s and 97.2 % at situation of pH (8); adsorbent dosage (0.8 for RTR and 0.6 for ATR), agitation speed (300 rpm), dye concentration (10 mg/L), temperature (298°K) and contact time (100 minute) respectively. The kinetics and equilibrium result of dye adsorption process well described by Pseudo 2nd order kinetic and Langmuir isotherm model respectively. The thermodynamic finding result shows the spontaneous and endothermic nature of the sorption process. The probable adsorption mechanism of MB dye on the prepared bio adsorbents surface may be assigned mainly through chemisorption. The results of this study show, the current adsorbents promise an alternate green rout for treatment dye contaminated wastewaters.

Keywords: Bio-adsorbent, Chemical activation, Methylene blue dye, Operational parameter, Tella residue

In recent years, population growth, technological advances, industrialization, and the magnitude of these changes have produced large amounts of aqueous effluent to the natural environment, especially in the water bodies[1-4]. Water pollution is the greatest concern facing the world today. As a result, unsanitary conditions and poor water quality cause 3.1% death annually worldwide. Water is polluted by a variety of toxic chemicals from the printing, pharmaceutical, cosmetics, and leather, food and textile industries[5-8]. Of the various pollutants, dyes are the most troublesome pollutants, widely present in untreated wastewater of many manufacturing factories such as cosmetics, textiles, paper, leather, plastics and food industries, and cause widespread pollution of surface and groundwater resource in their area[2-4,6,7].

Manufacturing industries mainly textile, dyeing, printing, pesticide, coating paper, cosmetics, and pharmaceuticals use methylene blue (MB) dye for different applications[9-11]. Although, it is extremely toxic, carcinogenic and its degradation process is very challenging due to its aromatic ring[9, 11]. Consequently, its removal from aqueous effluent is notable activities in the scientific community. Different treatment methods have been practical over the past years for thetreatment of dye containing wastewaters. But, most of the treatment methods are ineffective for removal these dyes due to their extreme stability. From now, adsorption process becomes one of the most utilized method to treat the waste water which containing dyes by using different adsorbents[11-14].

In the existing time use of waste biomass solid as adsorbents has established especial interest in the scientific community due to their obtainability, high selectivity, low charge, and efficacy[6,7,15]. Based up on this evidence the following materials were castoff as adsorbent for waste water treatment which containing methylene blue dye**.** These are: Raw wood ash[16], acid activated wood ash[16], beneficiated wood ash[16], Banana stem[9], Sugar Scum[17], fava bean peel waste[18], potato leaves and stems[19], Butea monosperma leaf[2], red kaolin[20], Ficus Nitida leaves[21], soya waste[22], etc.

Currently, new materials with fascinating adsorption capacity are discovered every year. In this study, we used conventional fermented beverage tella residues as a low-cost bio adsorbent**.** Tella is often homemade liquor and one of the oldest traditional alcoholic beverages, in almost every local state of Ethiopia. It is commonly consumed on holidays, annual celebrations, special festivals and church ceremonies in large amount. It is known as local beer because it is a malt-based drink like the commercial beer[23]. Various grains like that of wheat, barley, rice, sorghum, teff and auxiliary ingredients such as powdered stems and leaves of Gesho (Rhamnus prinoides), malt, and water are used for production of tella[23]. According to S.S. Pandiella *et al*. reports[24], cereals are grownup in 73% of the world's total crop space and provide more than 60% of the world's food fabrication by given that the fiber, protein, energy, minerals and vitamins needed for human wellbeing. It is also cultivated throughout Ethiopia and harvested in large quantities. Natural polymers such as starch, water-soluble dietary fiber, insoluble components of dietary fiber, and some free sugars are the main chemical component of grain[24]. The major composition of cereals such as barley, wheat and maize are starch. As reported by[25], grain carbohydrates, primarily starch, are the most abundant sources of energy. In Ethiopia, the stems and leaves of the gesho plant (Rhamnus prinoides) are used to give and preserve the typical bitterness and aroma of drinks. Because of leaf part contains various phenolic compounds such as naphthols, anthraquinones, flavonoids, and their glycosides[26-28]. As a general, the stem part of pants including Ethiopian Gesho (Rhamnus prinoides composed from cellulose and other components with the natural polymer lignin as a binding agent. These chemical compositions present in grain and in the auxiliary substances serves as a carbon basis for the generation of bio sorbent from the tella residue (atella). Wheat or barley used to make malt to accelerate the fermentation of the grain. Large amounts of water are used to prepare raw materials, wort (tinsis), and for dilute of fermented beverages.

The detailed process is mainly by blending powdered malt and Ramnus prinoides leaf and stem powder with water as a solvent in a closed container and holding for 3-5 days depending on the environmental conditions. This is also known as wort preparation. Secondly, powdered roasted cereals are mixed with wort and small amount of water as a solvent on the other closed container and allowed for fermentation to undergo. After a week, the fermentation product is diluted with sufficient water and filter liquid beer (tella) for drinking and discarded solid mass residue (atella) as byproduct. According to Nigusie Megersa literatures reports[29], in Addis Ababa over two million hectoliters of tella is produced per annum in the households and tella vending houses and he used the tella residue for the subtraction of pesticides from polluted water. At the present time tella is produced in different rural as well as urban area of Ethiopia and huge amount of solid residue called 'atella' disposed as a byproduct. Therefore the current study focused on the utilization of tella residue (atella) for the deletion of MB dye from artificially contaminated water.

Experimental Section

Chemicals

MB dye and other chemicals utilized in this study were analytical reagent grade which obtained from sigma Aldrich and used intrinsically without further cleansing. MB is analytical reagent (AR) grade (chemical formula $C_{16}H_{18}N_3SCl$; FW: 319.86 g/mol; λmax: 665 nm) and water soluble solid powder. Pure water was wont to make all solutions. Stock solution (500 mg/L) was prepared by dissolving a measured amount (0.5g) of dye powder in pure water and other working and standard solutions were prepared by dilution process from the stock solution. UV-Vis spectroscopy was used to resolve the utmost wave length of MB dye by taking known concentration of dye and with scanning from 200-800 nm range.

Adsorbent production

The bio adsorbents were produced according to[6,7,29] with little modifications. Tella residue (atella) was collected from Bahir Dar city, Ethiopia, locally referred to as tella vending houses. The sample was washed with H_2O to get rid of water soluble foreign materials within the sample.The resulting residue was sun dried for 3 days and then oven dried at 105°C for 4 h. Secondly,it was milled by ball miller and sieved

by manually shaking stainless-steel mesh screens with the opening of normal 1 mm sieve size and physically activated by carbonization in a muffle furnace (Nabertherm B180) for 2 h at 400°C in the absence of air. Then after, chemical activation carried out after the sample allowed cooling down for some minutes. Due to synergistic effect, the reaction between carbon–oxygen and the alkaline bond, alkaline process was used to totally expose the active adsorption sites and to increase functional groups of the adsorbent[30-33]. It was carried out by mixing powdered sample with 1N of NaOH in a mass ratio of (1:5) and shaking for 12 h. The resulting sample was filtered and washed with 2N of HCl /water several times until the *p*H reached to neutral. Finally, the prepared bio sorbent was dried at 110°C in oven for 3h to obtain good carbon structure and large surface area and kept in sample holder for next study.

Adsorbent characterization

Adsorbent properties such as ash content, moisture content, bulk density, volatile matter , fixed carbon, *p*H and pH_{PZC} were assessed based on the method used by previous scholars[6,16, 34, 35] with minor changes. Brunauer-Emmett-Teller surface area analyzer, BET (NOVA 4000e) was used to measure the surface area and pore parameters of the bio adsorbents. FTIR spectroscopy (JASCO-FT/IR-6600A) was used to detect the surface functional group of the bio adsorbents upon scanning on the wavelength range of 400–4000 cm^{-1} with firmness of $0.4cm^{-1}$. The surface morphology of the bio adsorbents were determined by scanning electron microscope, SEM (JEOL-5800LV) at an accelerated voltage of 10 kV and 3400x magnification. The thermal degradation/steadiness of the sorbents was examined using thermo gravimetric analyzer, TGA (BJHENVEN: HCT-1) with the help of nitrogen gas flow rate of 50 mL/min.

Point of zero charge (pH_{ZPC}) estimation of both adsorbents were performed based on solid addition method[6,19,36]. pH_{PZC} of an adsorbent could be a vital characteristic that tells the *p*H at which the adsorbent surface has net electrical neutrality. To search out pH_{Zpc}, the experiments were conducted by adding 0.1 g of adsorbent to 50 mL of 0.1 M NaCl solution in different container and adjust *p*H from 2 to 13 successively with agitated on a magnetic stirrer. Then, after the final *p*H of the solutions were measured after 24 h and the curve that cuts the pH_0 line of the plot final *p*H vs pH_0 tells pH_{ZPC} of the adsorbent.

Adsorption experiments

Batch adsorption experiments were conducted based on the method utilized by[21,37-39] with minor changes. The impact of operational parameters like initial dye concentration (10–60 mg/L), *p*H (2–12) , adsorbent dose (0.2-1 g), contact time (10-140 min), Temperature (25-45°C), and agitation speed (150-400 rpm) on the removal of MB dye were considered in a batch mode of operation. A known concentration dye sample (50 mL) was added in to 250 mL of conical flask followed by addition of 0.2g adsorbent and the required solutions *p*H was adjusted with 0.1M HCl or 0.1M NaOH for batch experiment. Consequently, the mixtures were agitated with magnetic stirrer on digital hot plate at 200 rpm until the desired time reached. Dye adsorbed adsorbent was separated from solution by centrifugation at 4000 rpm for five minute and absorbance of supernatants solutions were measured by using UV-Vis spectro-photometer at a maximum wave length of 665 nm. The equilibrium adsorption capacity, qe (mg/g), removal efficiency (%) were calculated by equation described on[21, 37-39] with their usual meanings. Different kinetics model (pseudo 1st order, pseudo 2nd order and interparticle diffusion model) and isotherm models (Langmuir, Freundlich and temkin) were applied to analyze the dye adsorption process.

Results and Discussion

Bio adsorbent properties

The proximate analysis and BET analysis results of both raw (RTR) and activated (ATR) tella residue bio adsorbents were displayed in Table 1. As stated in the Table l, RTR have very high moisture, ash, and volatile matter as compare to ATR bio sorbent which is due to the fact that in physiochemical activation process, organic substance mainly volatile matter and heat sensitive molecules are released as gas and liquid

Table 1 — Physiochemical properties of bio adsorbents

Sample	AM (%)	AA (%)	AVM (%)	AFC (%)	BD (g/mL)	pH	pH_{ZPC}	SA (m^2/g)	Pore volume (cc/g)	Pore size (Å)
RTR	9.32	16.72	27..35	46.62	0.52	6.76	6.33	51.32	0.0756	1.754
ATR	2.12	8.92	13.67	75.29	0.63	7.82	7.48	565.00	0.1444	16.89

AM: Amount of moisture, AA: Amount of Ash , AVM: Amount of volatile matter, FC: Fixed carbon, BD: Bulk density, SA: Surface area

products which enhance the carbon content of ATR[16,40]. The very low moisture content for ATR is corresponded to the loss of adsorbed water during physiochemical activation process. Per different scholar finding chemical activation process drops the ash content and decomposes the tissue of the carbon precursor which creates some new pores and voids which enables for adsorption of contaminants to itself[41-44]. The *p*H of RTR and ATR was found to be 6.72, 7.53 respectively. As reported by[40] for many applications, carbon *p*H 6–8 is appropriate. Therefore, *p*H values obtained in this study are in the range of adequate limit. Determination of filterability and floatability property of the adsorbent in terms of the physical parameter bulk density is very important[45-47]. It suggests that if the activated carbon is added to water it'll sink which with lead to better contact with the adsorbate and thereby resulting in effective adsorption process[45-47]. The result indicates ATR have high bulk densities than RTR due to the presence of high fixed carbon content. Thanks to physiochemical activation process, surface area, pore volume and pore size of ATR (565m^2/g, 0.1444 cc/g and16.89 Å) were much above RTR (51.32 m^2/g, 0.0756 cc/g and 1.754 Å). The physiochemical treatment was able to assists for the formation of porous adsorbent which increasing the extent of adsorption contaminants[48].

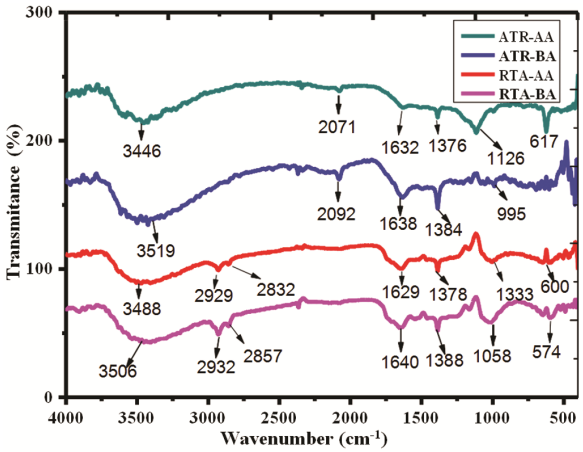

Fig. 1 — FTIR spectra of RTR and ATR pre and post MB dye adsorption (ATR-Activated tella residue, RTR-raw tella residue, BA-before adsorption and AA-after adsorption).

FTIR analysis was wont to work out for detection of some surface functional groups of the bio adsorbents for pre and post dye adsorption process (Fig. 1). As stated on the Fig.1 for both adsorbents the broad peak around 3440-3506 cm^{-1} relates to the O–H stretching vibration of alcohols, phenols and carboxylic acids as in pectin, cellulose, and lignin, thus showing the presence of ‘‘free’’ hydroxyl groups on the adsorbent surface[7, 49, 50]. For RTR the bands within 2932-2857cm^{-1} attributed to symmetrical stretch vibration of C-H for aliphatic hydrocarbon. The peak in the range of 1700-1640 cm^{-1} and 1400-1388 cm^{-1} were likely due to C=O stretching of carboxylic acid and C=C stretching vibration of aromatic ring bands respectively. The peak detected at range of 1300-1000 cm^{-1} and 600-700 cm^{-1} were titled to C-O bonds stretching and aromatic and furfural C-H out of plane bending vibration[51]. The peak detected in the range of 550-600 cm^{-1} might be related to phenyl group. On the opposite hand, similar spectra were observed for ATR with the exception of intensity difference and disappearance of spectra at range of 2932-2857 cm^{-1}. This is due to the functional group chemically protonated/deprotonated and thermally unstable through physicochemical activation process which makes the intensity of the peaks altered[7]. Comparing the FTIR spectra pre-adsorption to those post-adsorption, it are often concluded that both peaks were shifted to the right after adsorption. This could be attributed to the

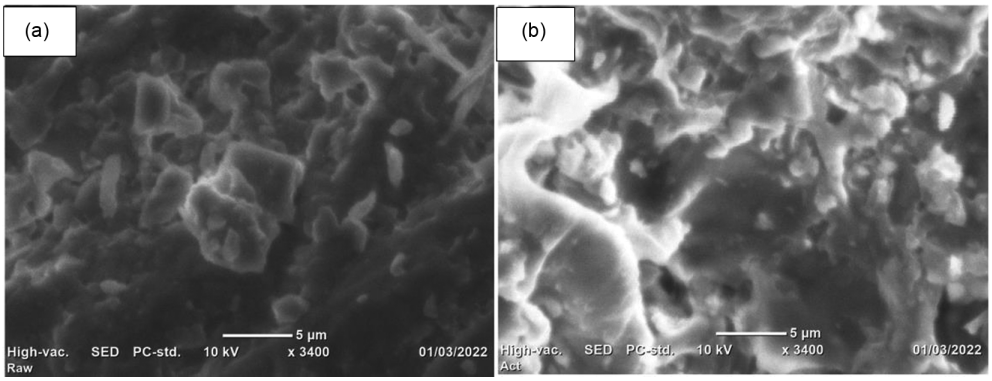

Fig. 2 — SEM image of (a) RTR and (b) ATR at 3400x magnification power.

adsorbent surface coverage by MB dye molecules through electrostatic interaction and hydrogen bonding between the dye molecule and adsorbents.

Scanning electron microscope (SEM) was utilized to detect surface morphologies of the bio adsorbents and the images are presented in Fig 2. As presented on the Fig. 2 the surface morphology of RTR has not visible pore, voids rather it is uniform surface. On the opposite hand, the surface morphology of ATR contains different visible pores, cracks, irregular shape and crevices as compare to RTR adsorbent. This can be due to volatile matter and other heat sensitive molecule released during chemical activation process[53]. This result was also checked with BET analysis. As stated on BET analysis result, physiochemical activation process stimulates the formation of porous structure and better surface in ATR. As stated by[49], these surface properties of the adsorbent enables as active site for dye removal process.

Thermo gravimetric analysis (TGA) is the most widely used method for assessing the thermal stability of a particular sample[8]. TGA plots of RTR and ATR (Fig. 3) shows the continuous weight loss at approximately 250°C for RTR and 370°C for ATR associated with the release of heat-sensitive molecules such as volatile organic compounds and moisture which adsorbed on both the surface and pores of the bio adsorbents[8, 54]. In the first phase, RTR weight loss is greater than ATR. This is due to the presence of more water and volatiles, as confirmed by the proximate analysis results. Secondly, the mass loss at 250-400°C temperature range for RTR and 300-400°C for ATR represents the decomposition of cellulose and hemicellulose. Moreover, in this temperature range, the mass loss of the ATR is greater than that of the RTR. This can be a bond relaxation of ATR during pyrolysis and chemical activation processes, facilitating material loss. At temperatures above 400°C, biomass loss may indicate a decrease in lignin weight[55]. No further detachment was recorded at temperatures above 650°C, indicating char formation[54].

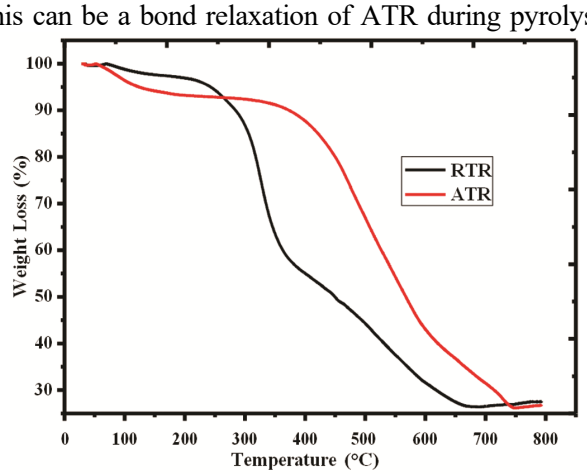

Fig. 3 — Thermo gravimetric (TG) curve of the RTR and ATR of bio adsorbents.

Factor affecting adsorption process

As stated by many scholars[11-14] , the dye sorption process is predominantly influenced by the physio-chemical properties of the adsorbent and the conditions where adsorption takes place. Consequently, it is important to understand the impact of these individual factors in dye adsorption process. Adsorption conditions such as adsorbent, contact time, initial solution *p*H, dose, agitation rate, reaction temperature, and initial MB concentration were estimated in this study.

***P*H$_{ZPC}$ and effect of solution *p*H**

Adsorbent *p*H$_{ZPC}$ is essential parameter that governs the pH at which the surface of the adsorbent reveals the presence of equal negative and positive charge (electrically neutral). So, adsorbents generate a negative charge when the *p*H is above *p*H$_{ZPC}$ and a positive charge when the *p*H is below *p*H$_{ZPC}$. As shown in Fig. 4, the *p*H$_{ZPC}$ values for RTR and ATR were 6.51 and 7.32, respectively. This result is close to the *p*H of both aqueous adsorbents. The *p*H value has a vital role in the adsorption of dyes on materials[19, 55]. To examine the impact of solution *p*H on MB dye removal from aqueous solution by raw (RTR) and activated (ATR) tella residues the experiment were assessed at various *p*H(2 -12), initial dye concentration (10 mg / L and 20 mg /l), contact time (40 minutes), adsorbent dose(0.2g), temperature (298°K) and stirring speed (200 rpm) and presented in Fig. 5 (a). As can be seen from the Fig. 5, the removal rate of MB by both

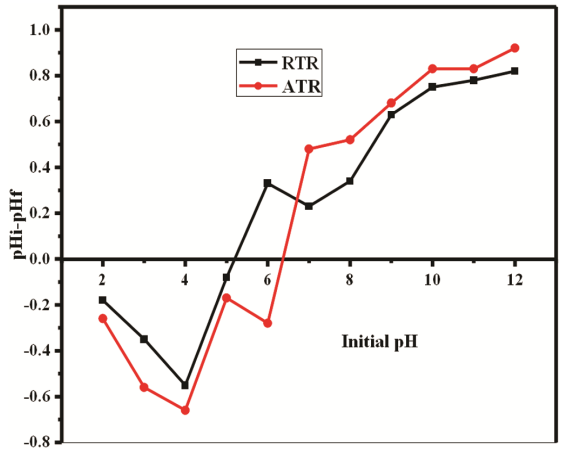

Fig. 4 — Point of zero charge (*p*H$_{zpc}$) for the prepared bio adsorbents.

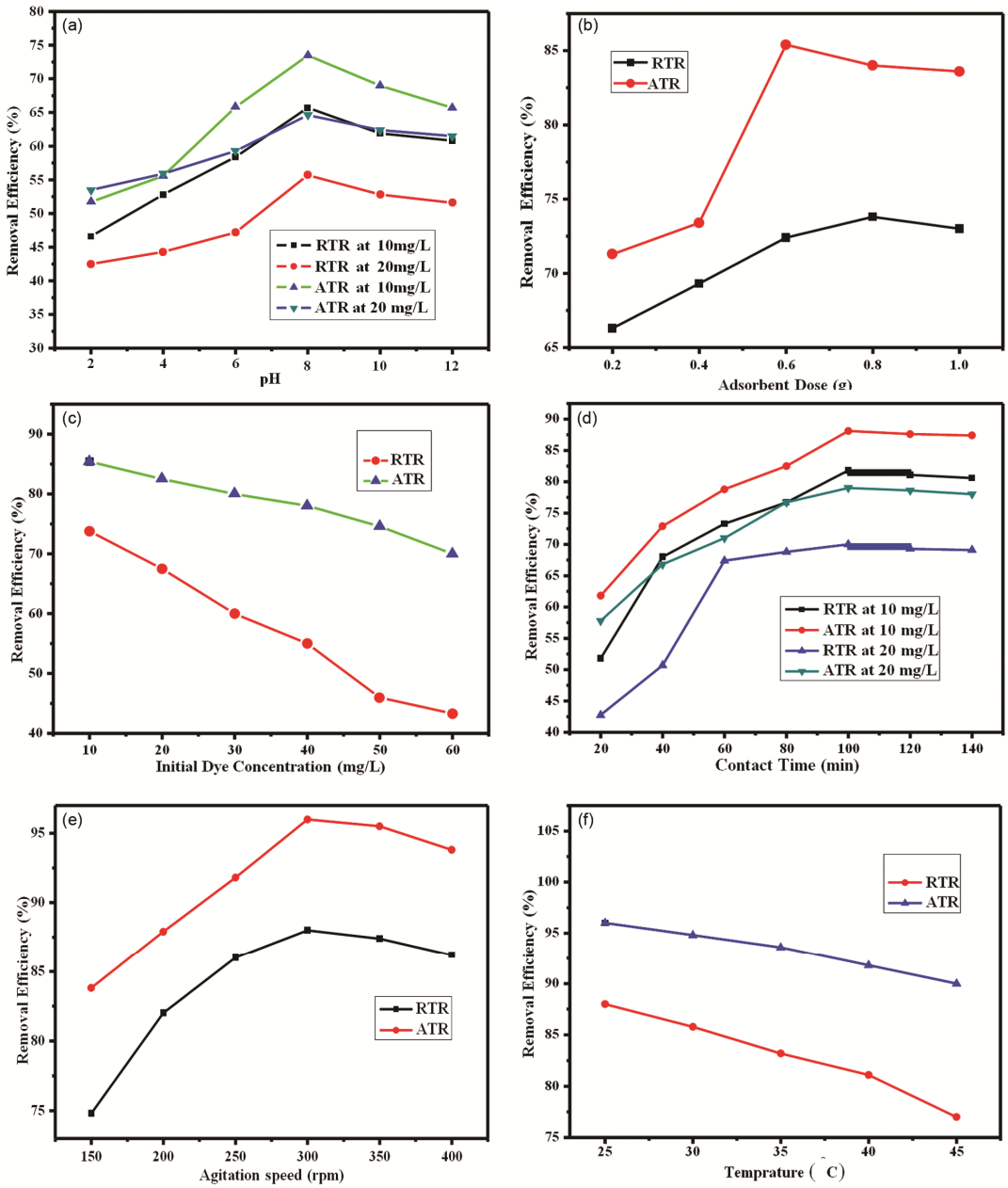

Fig. 5 — (a) Impact of solution *p*H on methylene blue dye using RTR and ATR as an adsorbent; (b) Impact of bio adsorbent load on the removal of MB dye by RTR and ATR; (c) Impact of initial MB dye concentration on its removal by RTR and ATR bio adsorbents; (d) Impact of contact time on removal MB dye by RTR and ATR as an adsorbent; (e) Impact of agitation speed on methylene blue dye removal by the prepared adsorbents and (f) Impact of solution temperature on the removal of methylene blue dye by the prepared adsorbents at optimum condition of other parameters.

adsorbents increased as the *p*H rises from 2 to 8 for both concentration ranges and the optimum removal attained at *p*H 8 which was selected for the subsequent experiments. This is the fact that an increase in *p*H leads to deprotonation of adsorbent surface which forms negative charge and enhance adsorption process through electrostatic interaction towards the positively charged dye molecule[56, 57]. Conversely, at low *p*H (acidic medium), there is an excess hydronium ions which computes with positively charged dye molecule on available active site of the adsorbents[21, 58]. On the other hand, the amount of adsorption changed slightly when the *p*H was higher than 8 for both adsorbents due to the high computation of hydroxyl group with active site of adsorbents for the uptake of adsorbate molecules.

Impact of adsorbent dose

Measureable adsorbent dose determination of the model adsorbent is required. In fact, increasing the adsorbent dose improves adsorption efficiency due to the increasing in the number of active site on the adsorbents[6, 39]. Figure 5 (b) shows the change in removal efficiency of MB dye with varying adsorbent dosage (0.2 to 1 g) at initial dye concentration of (10 mg /L), contact time (40 min), temperature (298°K.), stirring rate (200rpm) and *p*H 8 for both adsorbents. As stated in Fig. 5 (b) , percentage of MB dye removal increases as the adsorbent dose is increased from 0.2 to 0.6 g for ATR and 0.2 to 0.8 g for RTR. At masses over 0.8 g for RTR and 0.6 g for ATR, the amount of MB dye removal is slightly decreased due to the aggregation and overlap of adsorbentparticles in the solution, and the mass ratio between the active site and the adsorbent is reduced which leads to decreasing in adsorption[6,39].

Initial dye concentration effect

To know the impact of dye concentration on removal of MB by the bio adsorbents (RTR and ATR), the experiments were undergo by varying MB dye concentration(10 - 60 mg / L) at contact time (40 minutes),room temperature, stirring rate (200 rpm) and under optimal conditionsof other optimized parameters and the result is presented on Fig. 5 (c). As stated in Fig. 5 (c), additional concentration of contaminants lead to reduced removal rates due to saturation and limitation of the binding site of the adsorbent. As the load of contaminants increases, more and more of these molecules are adsorbed on the surface of the adsorbent and become unable to react with the remaining target molecules due to repulsion between adsorbate present on adsorbent surface with adsorbate present of the solution phase[59]. A relatively high level of sorption was observed when the initial concentration of MB dye was low. This is due to the high ratio of available binding sites to dye molecule present which makes small number of dye molecules competing for the available binding sites[57, 60, 61].

Impact of contact time

Adsorption contact time helps to regulate the potential initiation of binding and the optimal timefor contaminant removal in real-world applications[3, 62]. To examine the impact of contact time on the percentage removal of MB by the RTR and ATR, experiments were tested at different time intervals (20-140 minutes) with adsorbent dose (0.6 g for ATR, 0.8 g for RTR), pH 8 for both adsorbents, in a room temperature and stirring speed of 200 rpm and is shown in Fig 5 (d). Time plots show that adsorbents removal are rapid for the first 60 minutes, but gently slow down up to equilibrium point is reached. Because of a large number of empty active sites are available in the early stages, and over time it is difficult to fill the remaining empty surface sites which is attributed to the repulsive power between the solute molecule present in solution and in the bulk phase[63, 64]. Equilibrium was reached after shaking for 100 minutes for both adsorbents and after the stability time reached the MB adsorption process was fixed over time.

Agitation speed

The impact of agitation speed on adsorption effectiveness has also been studied because it affects the distribution of solutes in all solutions and the formation of outer boundary membranes[65-67]. To examine the impact of agitation speed on MB dye removal by the prepared bio adsorbent, experiments were performed at various stirring speeds (150-400 rpm) using other optimum conditions specified at room temperature and presented in Fig. 5 (e). As shown in Fig. 5 (e), increasing the agitation speed from 150 to 300 rpm can increase the proficiency of MB dye removal and gradually decreasing its removal. These phenomena due to increased migration can increase the dynamic migration of dye molecules towards the adsorbent surface, and excessive increases can lead to dissolution of the adsorbate from the adsorbent surface.

Effect of temperature

Under optimal conditions of the parameters determined above, the influence of temperature (298-318 Ok) on the removal rate of MB dye by the produced adsorbents has been optimized, and the results are presented in Fig. 5 (f). As indicated in Fig. 5 (f), as the temperature climbedfrom 25 to 45 ° C, the MB dye removal rate reduced from 87.2 percent to 77 percent and from 97to 90 percent for RTR and ATR, respectively. This decrease in adsorption efficiency with rising temperature is likely due to the weakening of the physical link between the dye (adsorbate) and the active site of the adsorbent as the temperature rises. Furthermore, the dye's solubility is improved, and the interaction between the solute and the solvent is stronger than that between the solute and the adsorbent which makes adsorption of solutes becomes harder[68-70].

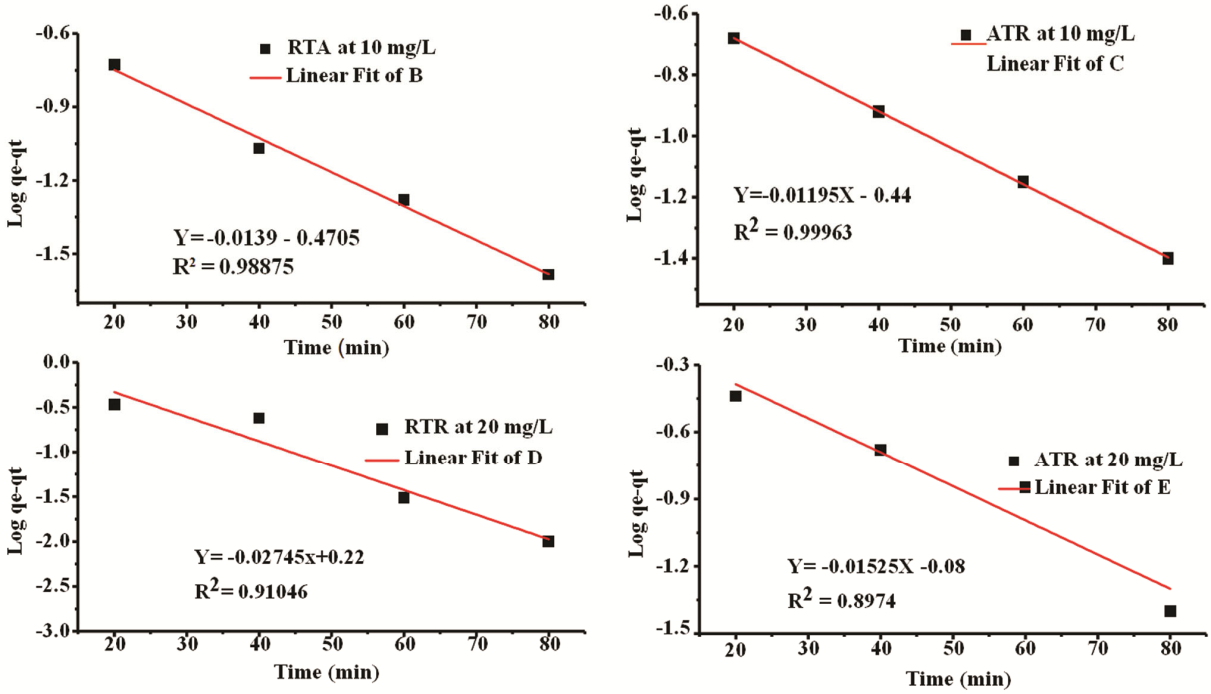

Fig. 6 — Pseudo 1st order kinetics graph for RTR and ATR at different contact time (20- 80 min.), room temperature, 200 rpm agitation speed and optimum condition of other optimized parameters.

Table 2 — kinetics paramours obtained from the corresponding kinetics graph

Kinetic models	parameters	RTR		ATR	
		Concentration(mg/L)			
		10	20	10	20
	qe exp.	0.51	0.87	0.73	1.2
Pseudo 1st order	R^2	0.98875	0.91046	0.99963	0.8974
	K_1 (min^{-1})	-0.0139	-0.02745	-0.0119	-0.01525
	qe cal.(mg/g)	0.34	1.66	0.37	0.83
Pseudo 2nd order	R^2	0.99772	0.98373	0.99766	0.99776
	qe cal. (mg/g)	0.56	0.96	0.757	1.41
	K_2(gmg^1min^{-1})	0.137	0.07452	0.154	0.0723
Interparticle diffusion model	R2	0.82697	0.68505	0.80262	0.86773
	Kdiff	0.02374	0.34478	0.02553	0.04852
	C (mg/g)	0.26467	0.38906	0.44019	0.79091

Adsorption kinetics

Kinetic studies are significant because they aid in determining the applicability of adsorption mechanisms and give data to aid in the design of experimental techniques. Fast adsorption rates and short adsorption durations are required for a variety of applications such as decolorization, wastewater treatment, and organic pollutant removal. To better comprehend the adsorption rate of current research, the linear forms of the equations of the first-order pseudo-model, the second-order pseudo-model, and the interparticle diffusion model with the normal meaning are adopted from[3, 62, 71]. The response rate constants k and qe for each model are derived using the graphs of log (q_e-q_t) versus t for the pseudo 1st order model, t/qt versus t for the pseudo 2nd order model, and q_t versus $t^{1/2}$ for the interparticle diffusion model and the graphs shown in Figs 6, 7, and 8 respectively.

The feasibility of these models is determined by assessing their respective correlation coefficients (R^2) and the agreement between experimental and estimated q_e values. Table 2 shows the correlation coefficients (R^2) and the parameters associated with

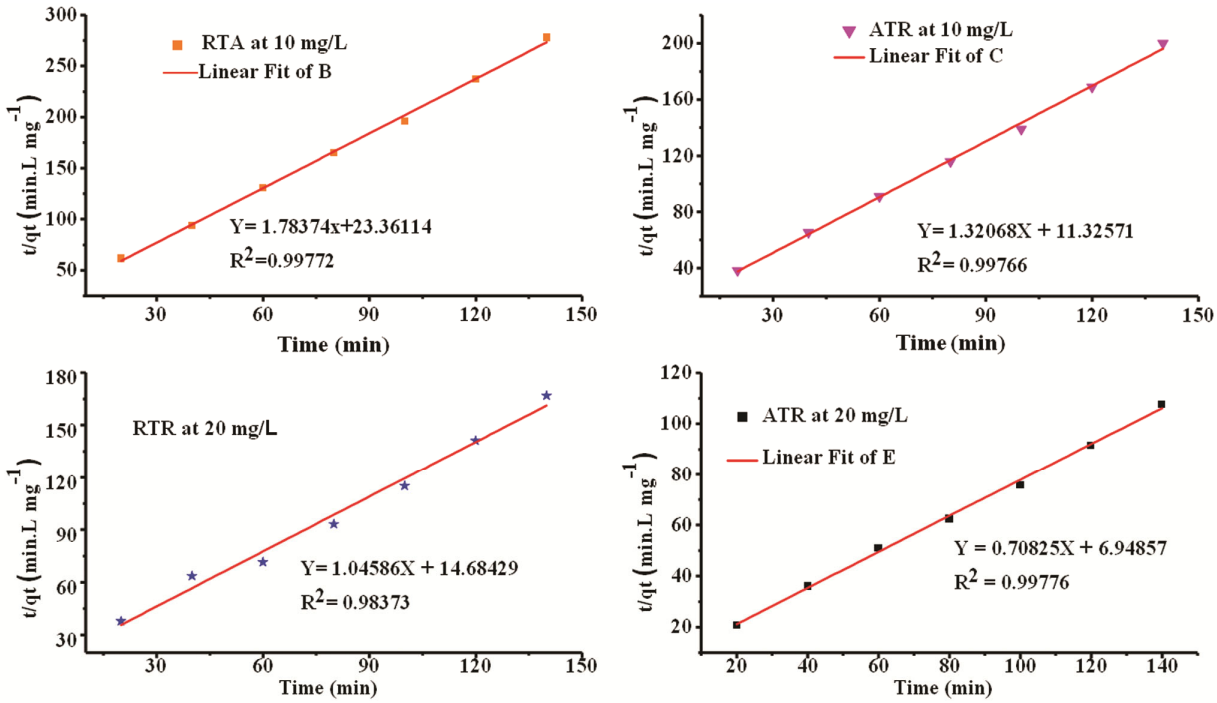

Fig. 7 — Pseudo 2nd order kinetics graph for RTR and ATR at different contact time (20- 80 min.), room temperature, 200 rpm agitation speed and optimum condition of other optimized parameters

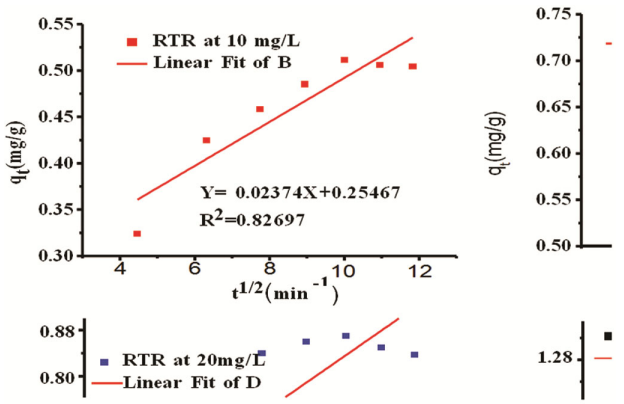

Fig. 8 — Interparticle diffusion model graph for RTR and ATR at different contact time (20- 80 min.), room temperature, 200 rpm agitation speed and optimum condition of other optimized parameters.

each model, which are computed from the corresponding kinetics graph using their linear form of equations which described on the literatures[3, 62, 71]. In terms of correlation coefficient, the pseudo second order kinetic model fit the experimental data much better than the pseudo first order and interparticle diffusion kinetic model. In addition, the value of qe obtained from the quadratic pseudo 2nd model is comparable to the investigational value of q_e compared to other dynamic models. As reported in[5, 63], as a very general guide, the process is usually kinetic controlled ifequilibrium is reached within 3 h and if it reaches 24 h or more it becomes diffusion kinetics control. The C value of the interparticle diffusion model is higher in ATR than in RTR, signifying that the surface sorption of MB to the ATR bio adsorbent is strong. Because of the close fit to the PSO model, chemisorption appears to be the rate-determining phase in the adsorption process. The mechanism in this situation is valence forces resulting from electron sharing or exchange between the adsorbent and the adsorbate[63]. At low concentrations, the K_2 value is higher than at high concentrations. This is due to competition for the active site of the adsorbent between large quantities of MB species[63].

Thermodynamic studies

To determine the spontaneity of the sorption process, thermodynamic characteristics must be considered. The effect of temperature on the process is indicated by changes in Gibbs free energy (ΔG◦), solubilization enthalpy (ΔH◦), and entropy (ΔS◦) values. The system's ΔS◦ and ΔH◦ must be measured to derive the Gibbs free energy of the process[63, 72, 73]. Van't Hoff's equation[63] was used to calculate these parameters. As is customary, the graph is plotted as $\ln K_C$ versus 1/T (K^{-1}) and shown in Fig. 9.

Table 3 — thermodynamics parameters for MB sorption onto RTR and ATR

Type ofadsorbent	Temperature(K)	Thermodynamics			
		lnKc	ΔG° (kJ/mol)	ΔH° (kJ/molK)	ΔS° (J/mol K)
ATR	298		-1709.524	-39658.988	-127.283
	303		-1083.231		
	308		-563.357		
	313		572.502		
	318		1057.540		
RTR	298		1932.506	-25315.416	-91.453
	303		2367.993		
	308		2867.997		
	313		3226.830		
	318		3886.462		

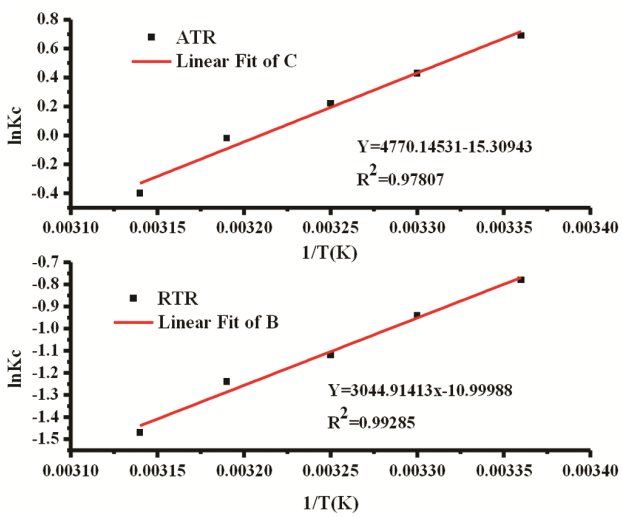

Fig. 9 — Plot of ln (Kc) vs 1/T for examine of thermodynamic parameters for the adsorption ofMB onto RTR and ATR.

A negative value of ΔG◦ in ATR (Table 3) indicates that MB is adsorbed well and spontaneously by the bio adsorbent without the need for additional energy. With increasing temperature, a small negative value of ΔG◦ suggests that the adsorption process is less advantageous at high temperatures and preferable at low temperatures[72]. A positive value of ΔG° in RTR indicates that the adsorption of MB on this adsorbent was not spontaneous. The negative sign and magnitude of ΔH° indicate that the adsorption process is exothermic and that hydrogen bonds and dipole interactions play a role in the adsorption process. The exothermic nature of the adsorption process suggests that dye species penetration into the adsorbent's interior pores may not be a significant factor in the adsorption process. A negative ΔS◦ value on the other hand, indicated a decrease in randomness at the solid solution interface. With increasing temperature, dye molecules become more mobile, and adsorbed species desorb from the solid to the liquid phase[63, 72]. As a result, in the higher temperature ranges, the amount of MB absorbed by the bio adsorbent reduced.

Adsorption isotherms

Adsorption isothermal studies are crucial because they help to explain the interaction between adsorbents and adsorbents. It can also be used to figure out the adsorption capacity[30, 36,74]. Adsorptions isotherms can be modeled in a variety of ways. To analyze the MB uptake equilibrium for varied MB concentrations on tella residue bio adsorbent, the Langmuir, Freundlich, and Temkin isotherms were chosen. Their underlying assumptions, the shape of the isotherm, and the type of the adsorbent surface are what set them apart. The Freundlich isotherm assumes a heterogeneous surface with a non-uniform heat of adsorption distribution over the surface, whereas the Langmuir assumes that sorption occurs at specified homogeneous locations inside the adsorbent[48, 75]. Because of adsorbent adsorbate relationships, the temkin isotherm assumes that the adsorption heat of each molecule in the layer falls linearly with coverage. It also assumes that up to the greatest binding energy, the adsorption is characterized by a comparable distribution of binding energies[58]. To examine the equilibrium data, the linear form of equations for such models are chosen from[30,36,74] with their typical meanings. The isotherm curves were produced as normal, using Ce/qe versus Ce for the Langmuir isotherm, logqe vs log Ce for the Freundlich isotherm model, and qe versus lnCe for the Temkin isotherm and presented in Fig. 10.

The intersections and slopes of the Ce/qe versus Ce plots can be used to estimate Langmuir isotherm parameters such as qm and b model respectively. K_f and n values for Freundlich isotherm can be estimated from the intercept and slope of log qe versus log Ce graph. The slope and intercept of qe versus ln Ce plot

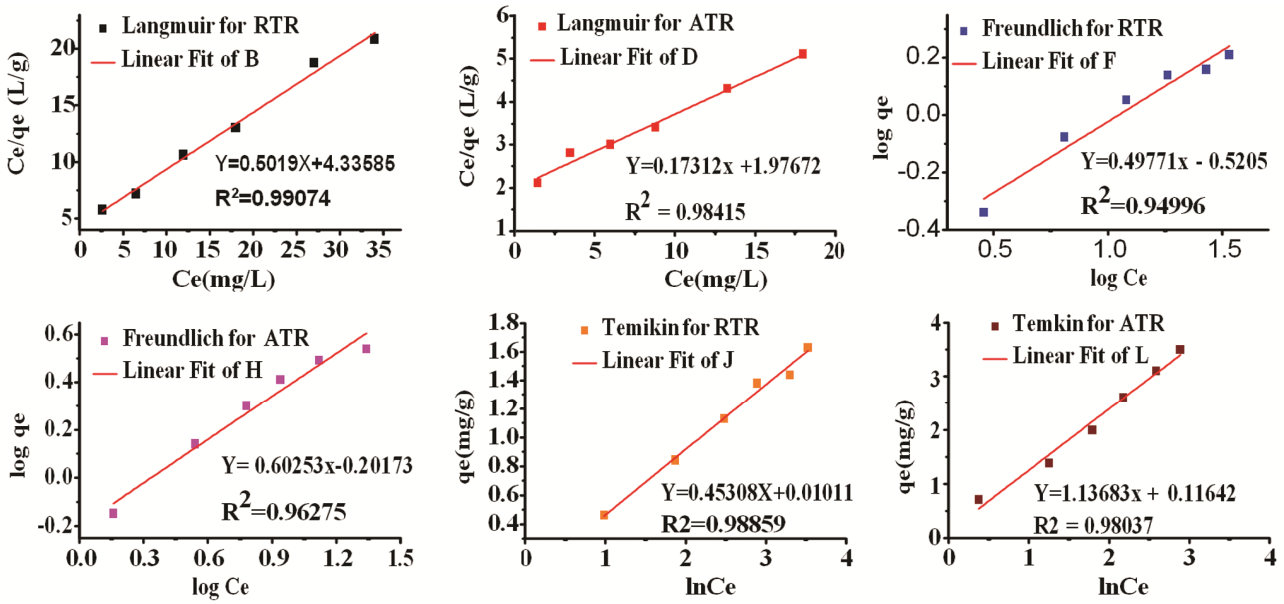

Fig.10 — Langmuir, Freundlich, and Temkin isotherm models at various MB dye concentrations (10-60 mg/L), adsorbent dosage (0.8 for RTR and 0.6 for ATR), *p*H (8), and contact period (60 minute), 200 rpm stirring rate and room temperature

Table 4 — Isotherm parameters determined from the isotherm plot

Isotherm models	Parameters	RTR	ATR
Langmuir	R^2	0.99074	0.98415
	q_m (mg/g)	1.990	5.780
	b(L/mg)	0.116	0.087
Freundlich	R^2	0.94991	0.96275
	K_f(mg/g)	0.301	0.628
	N	1.92	1.66
Temkin	R^2	0.98859	0.98037
		0.45308	1.13683
	A(L/g)	2.210	0.990
	b(J/mol)	5468.290	2179.37

were used to estimate the value of β and A in the Temkin isotherm. Correlation coefficient (R^2) and isotherm parameters calculated from the isotherm graphs are reported on Table 4 below.

The reliability of the adsorption isotherm model can be examined by the value of the regression coefficient (R^2) and the adsorption capacity determined from the isotherm plot. Correlation Coefficient (R^2) for each model indicates the suitability of the experimental data. The R^2 value of a model close to 1 is measured as the most suitable and optimal model for adsorption[2]. The Langmuir isotherm regression coefficient (Table 4) values are close to 1 for both adsorbents. The agreement of these closes single regression coefficients proves that the Langmuir model of MB adsorption to the manufactured bio adsorbent is applicable and that the adsorption of MB to RTR and ATR was a single-layer adsorption process. The feasibility of Langmuir isotherm is cheeked by separation factor (R_L) which calculated from $R_L = 1 / (1 + b \times C_0)$. Somewhere b is the Langmuir constant associated to the intensity of adsorption(L mg^{-1}) and C_0 is the contaminant concentration (mg /L).This is an essential feature of the Langmuir isotherms, which virtually predicts whether the adsorption system is good and the calculated values at various concentrations are shown in Table 5 below. R_L <1 reveals promising adsorption, R_L > 1 disapproving adsorption, linear at R_L = 1 besides irreversible at R_L = 0 (Ref.16). Table 5 shows that the 1/n was between 0 and 1, and the R_L was less than 1 and showing that RTR and ATR adsorbents were good for adsorbing MB. Table 6 shows the performance of several adsorbents on methylene blue removal interims of monolayer capacity. As shown in the table, the current adsorbents have adsorption capabilities that are comparable to those of prior adsorbents.

Probable MB dye adsorption mechanisms

To understand the bonding mechanisms of contaminant with adsorbent surface, the nature of selectivity and sensitivity are obviously present on contaminant sorption process[4]. The sorption mechanism of MB is basically associated to the main chemical structures and active functional groups which depicted from FTIR analysis (-OH, C=C, -COOH, $-NH_2$) of the bio adsorbent used. At different solution pH, adsorbents surface generate charge which facilitates electrostatic

Table 5 — Values of the dimensionless constant separation factor (RL) at various beginningconcentrations

Adsorbents	R_L values					
	Concentration (mg/L)					
	10	20	30	40	50	60
RTR (0.8g)	0.463	0.301	0.223	0.177	0.147	0.126
ATR(0.6g)	0.535	0.365	0.277	0.223	0.187	0.161

Table 6 — Monolayer sorption abilities of various bio sorbent on MB dye removal.

Adsorbent	q_m(mg/g)	pH	Isotherm	Kinetic	Thermodynamic	Reference
RTR	1.99	8	L	PSO	Non-spontaneous	This study
ATR	5.78	8	L	PSO	spontaneous	This study
Waste ash	4.62	8	F	PSO	-	[16]
Coir pith carbon	5.72	6.9	L	PSO	Spontaneous	[76]
(Fe (III)/Cr (III) hydroxide)	5		Land F	PSO		[77]
Stem of Solanum tuberosum	41.6	7	F	PSO	spontaneous	[19]
Leaves of Solanum tuberosum	52.6	7	F	PSO	spontaneous	[19]
Hollow silica nanoparticles	64.06	8	L	PSO	spontaneous	[22]
Modified Cellulose Acetate membrane	88.2	6.5	L	I and PSO	spontaneous	[78]
Magnolia denudate waste leaf	185.19		L	PSO	spontaneous	[49]
Magnolia grandiflora waste leaf	149.25		L	PSO	spontaneous	[49]
Magnolia figo waste leaf	238.1		L	PSO	spontaneous	[49]
Malaysian low rank coal	421.1	10	F	PFO	-	[79]
Manganese-modified lignin bio char	161.81	11	L	PSO	-	[80]

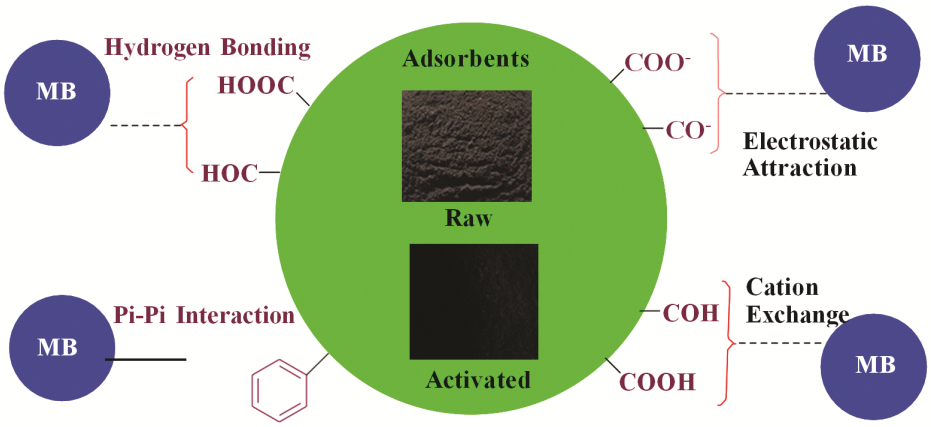

Fig 11— Possible adsorption mechanism of MB by the bio adsorbents

interaction with dye molecules. Various functional groups present of the adsorbent surface have a capacity to undergo ion-exchange reaction with MB dye molecule. The probable adsorption mechanism would be electrostatic interaction, ion exchange; pi to pi staking, physical adsorption and hydrogen bonding for adsorption of MB dye molecules onto RTR and RTR[81]. Figure 11 depicts a hypothetical adsorption method for methylene blue dye molecules on tella residue (atella) adsorbent materials.

Conclusion

The present study used a physiochemical activation approach to create a highly efficient bio sorbent from cereal-based tella residue, which was effectively evaluated for MB dye removal of from artificially polluted aqueous environment. In comparison to raw adsorbent, the SEM and BET results show that the physiochemical activation process aids in the production of a wide range of visible pores, fractures, irregular shapes, crevices, and a higher surface area

for ATR, which acts as an active site for dye adsorption. The results of current study reveal that various operational parameters such as solution pH, adsorbent dose, initial dye concentration, contact time, agitation speed, and temperature strongly affect MB dye sorption process. The equilibrium results were better described by the Langmuir model than to the Freundlich and Temkin isothermal models. The maximum dye bio sorption capacity of bio adsorbents are often compared to the reports in the literature. The kinetics study of MB dye removal by the tella-residue bio adsorbents were performed based on pseudo 1st -order, pseudo 2nd order, and intraparticle diffusion models. The results shows quadratic pseudo 2nd order model better describe dye sorption process. The thermodynamic study reveals the spontaneous and endothermic nature of the MB dye sorption process. In general, this finding reveals that the feasibility of physicochemically activated cereal based tella residue (atella) adsorbent as a promising material for decolorizing dye contaminated aqueous environment**.**

Acknowledgement

The authors express their appreciation to the Bahirdar University and Woldia University, Ethiopia for material support.

References

1 Hsini A, Essekri A, Aarab N, Laabd M, Ait Addi A, Lakhmiri R & Albourine A, *Environ Sci Pollut Res*, 27 (2020) 15245.
2 Das M, Samal A & Mehar N, *Int J Environ Sci Technol*, 17 (2020) 2105.
3 Mashkoor F & Nasar A, *J Magn Magn Mater*, 500 (2020) 166408.
4 Munjur H M, Hasan M N, Awual M R, Islam M M, Shenashen M & Iqbal J, *J Mol Liq*, 319 (2020) 114356.
5 Hoseinzadeh E, Samarghandi M R, McKay G, Rahimi N & Jafari J, *Desal Water Treat*, 52 (2014) 4999.
6 Abate G Y, Alene A N, Habte A T & Getahun D M, *Environ Syst Res*, 9 (2020) 1.
7 Alene A N, Abate G Y, Habte A T & D M, *J Chem*, 2021 (2021).
8 Patil C S, Kadam A N, Gunjal D B, Naik V M, Lee S W, Kolekar G B & Gore A H, *Sep Purif Technol*, 247 (2020) 116997.
9 Misran E, Bani O, Situmeang E M , Purba A S, *Alex Eng J*, 61 (2022) 1946.
10 Rostamian M, Hosseini H, Fakhri V, Talouki P Y, Farahani M, Gharehtzpeh A J, Goodarzi V & Su C H, *Chemosphere*, 289 (2022) 133219.
11 Almehizia A A, Al-Omar M A, Naglah A M, Bhat M A & Al-Shakliah N S, *Alex Eng J*, 61 (2022) 2386.
12 Xue H, Wang X, Xu Q, Dhaouadi F, Sellaoui L, Seliem M K, Lamine A B, Belmabrouk H, Bajahzar A & Bonilla-Petriciolet A, *Chem Eng J*, 430 (2022) 132801.
13 Lv B W, Xu H, Guo J Z, Bai L Q & Li B, *J Hazard Mater*, 421 (2022) 126741.
14 Liu H, Tian X, Xiang X & Chen S, *Int J Biol Macromol*, 202 (2022) 632.
15 Hussain Z, Chang N, Sun J, Xiang S, Ayaz T, Zhang H & Wang H, *J Hazard Mater*, 422 (2022) 126778.
16 Alene A N, Abate G Y & Habte A T, *J Chem*, 2020 (2020).
17 Elhadiri N, Bouchdoug M, Benchanaa M & Boussetta A, *J Chem*, 2018 (2018).
18 Bayomie O S, Kandeel H, Shoeib T, Yang H, Youssef N & El-Sayed M M, *Sci Rep*, 10 (2020) 1.
19 Gupta N, Kushwaha A K & Chattopadhyaya M, *Arab J Chem*, 9 (2016) 707.
20 Jawad A H & Abdulhameed A S, *Surf Interf*, 18 (2020) 100422.
21 Wang D, Wang Z, Zheng X & Tian M, *Indust Crop Prod*, 148 (2020) 112319.
22 Verma M, Dwivedi P K & Saxena N, *Colloids Surfaces A: Physicochem Eng Asp*, 587 (2020) 124333.
23 Berhanu A, Int Food Res J, 21 (2014)
24 Charalampopoulos D, Wang R, Pandiella S & Webb C, *Int J Food Microbiol*, 79 (2002) 131.
25 Rudi H, Uhlen A K, Harstad O M & Munck L *Animal Feed Sci Technol*, 130 (2006) 55.
26 Chen G L, Munyao M F, Xu Y B, Saleri F D, Hu G W & Guo M Q, *Pharmaceuticals*, 13 (2020) 55.
27 Amabye T G, *Ethiop Nat Prod Chem Res*, 3 (2015).
28 Nigussie G, Alemu M, Ibrahim F, Werede Y, Tegegn M, Neway S & Annisa M E, *Int J Second Metab*, 8 (2021) 136.
29 Megersa N, *Ethiop J Sci*, 38 (2015) 133.
30 Maia L S, da Silva A I, Carneiro E S, Monticelli F M, Pinhati F R & Mulinari D R, *J Polym Environ*, 29 (2021) 1162.
31 Garba Z N, Tanimu A & Zango Z U, *Bullet Chem Soc Ethiop*, 33 (2019) 425.
32 Pezoti O, Cazetta A L, Bedin K C, Souza L S, Martins A C, Silva T L, Júnior O O S,.Visentainer J V & Almeida V C, *Chem Eng J*, 288 (2016) 778.
33 Hamad B K, Noor A M, Afida A & Asri M M, *Desalination*, 257 (2010) 1.
34 Jaria G, Silva C P, Ferreira C I, Otero M & Calisto V, *J Environ Manag*, 188 (2017) 203.
35 Pal D B, Singh A, Jha J M, Srivastava N, Hashem A, Alakeel M A, Abd Allah E F & Gupta V K, *Bioresour Technol*, 339 (2021) 125606.
36 Malatji N, Makhado E, Ramohlola K E, Modibane K D, Maponya T C, Monama G R & Hato M J, *Environ Sci Pollut Res*, 27 (2020) 44089.
37 Uddin M K & Nasar A, *Sci Rep*, 10 (2020) 1.
38 Dao M U, Le H S, Hoang H Y, Tran V A, Doan V D, Le T T N & Sirotkin A, *Environ Res*, 198 (2021) 110481.
39 Abate G Y, Alene A N, Habte A T & Addis Y A, *J Polym Environ*, 29 (2021) 967.
40 Wang S & Zhu Z, *Dyes Pigm*, 75 (2007) 306.
41 Yorgun S & Yıldız D, *J Taiwan Inst Chem Eng*, 53 (2015) 122.
42 Lam S S, Liew R K, Wong Y M, Yek P N Y, Ma N L, Lee C L & Chase H A, *J Clean Prod*, 162 (2017) 1376.
43 Gunawan T D, Munawar E & Muchtar S, *Mater Today Proc*, 63 (2022).

44 Budianto A, Kusdarini E, Amrullah N, Ningsih E, Udyani K & Aidawiyah A, *Mater Sci Eng*, 1175 (2021) 012017.
45 Evbuomwan B & J Alalibo, *Chem Res J*, 2 (2018) 124.
46 Sugumaran P, *J Sust Energy Environ*, 3 (2012) 125.
47 Nakagawa Y, Molina-Sabio M & Rodríguez-Reinoso F, *Micropor Mesopor Mater*, 103 (2007) 29.
48 Bello O S, Adegoke K A & Akinyunni O O, *Appl Water Sci*, 7 (2017) 1295.
49 Guo D, Li Y, Cui B, Hu M, Luo S, Ji B & Liu Y, *J Clean Prod*, 267 (2020) 121903.
50 Rong X, Chen W, Huang Q, Cai P & Liang W, *Colloids Surf B: Biointerfaces*, 80 (2010) 79.
51 Venegas-Gomez A, Gomez-Corzo M, Macias-Garcia A & Carrasco-Amador J P, *Environ Chem Eng*, 8 (2020) 103561.
52 Chowdhury S, *Desalination*, 265 (2011) 159.
53 Subratti A, Vidal J L, Lalgee L J, Kerton F M & Jalsa N K, *Sust Chem Pharm*, 21 (2021) 100421.
54 Alamin N U, Khan A S, Nasrullah A, Iqbal J, Ullah Z, Din I U, Muhammad N & Khan S Z, *Int J Biol Macromol*, 176 (2021) 233.
55 Bouhadjra K, Lemlikchi W, Ferhati A & Mignard S, *Sci Rep*, 11 (2021) 1.
56 Sun Y, Gu Y & Yang J, *Chem Eng J*, 428 (2022) 131163.
57 Nordin A H, Ahmad K, Xin L K, Syieluing W & Ngadi N, *Mater Today Proc*, 39 (2021) 979.
58 Emara M M,.Farag R S, Mubarak M F & Ali S K, *Nanotechnol Environ Eng*, 5 (2020) 1.
59 Kamaraj M, Srinivasan N, Assefa G, Adugna A T & Kebede M, *Environ Technol Innov*, 17 (2020) 100540.
60 Biswas S, Mohapatra S S, Kumari U, Meikap B C & Sen T K, *J Environ Chem Eng*, 8 (2020) 103637.
61 Ahmad M A, Eusoff M A, Oladoye P O, Adegoke K A & Bello O S, *Chem Data Collect*, 32 (2021) 100676.
62 Mahi O, Khaldi K, Belardja M, Belmokhtar A & Benyoucef A, *J Inorg Organomet Polym Mater*, 31 (2021) 2095.
63 Sabar S, Aziz H A, Yusof N, Subramaniam S, Foo K, Wilson L & Lee H, *React Funct Polym*, 151 (2020) 104584.
64 Maleki A, Mohammad M, Emdadi Z, Asim N, Azizi M & Safaei J, *Arab J Chem*, 13 (2020) 3017.
65 Dod R, Banerjee G & Saini S, *Biotechnol Bioprocess Eng*, 17 (2012) 862.
66 Adesina O A, Taiwo A E, Akindele O & Igbafe A, *S Afr J Chem Eng*, 37 (2021) 23.
67 Adel M, Ahmed M A & Mohamed A A, *J Phys Chem Solids*, 149 (2021) 109760.
68 Enenebeaku C K, Okorocha N J, Uchechi E E & Ukaga I C, *Int Lett Chem*, 72 (2017) 52.
69 Akgül M & Karabakan A, *Micropor Mesopor Mater*, 145 (2011) 157.
70 Shaikh W A, Kumar A, Chakraborty S, Islam R U, Bhattacharya T & Biswas J K, *Chemosphere*, 291 (2022) 132788.
71 Elsherif K, Elsherif K M, El-Dali A, Alkarewi A A, Ewlad-Ahmed A M & Treban A, *Chem Int*, 7 (2021) 79.
72 Alver E, Metin A Ü & Brouers F, *Int J Biol Macromol*, 154 (2020) 104.
73 Priyadarshini B, Patra T & Sahoo T R, *J Magnes Alloys*, 9 (2021) 478.
74 Gharbani P & Mehrizad A, *Carbohydr Polym*, 277 (2022) 118860.
75 Deng H, Lu J, Li G, Zhang G & Wang X, *Chem Eng J*, 172 (2011) 326.
76 Kavitha D & Namasivayam C, *Bioresour Technol*, 98 (2007) 14.
77 Namasivayam C & Sumithra S, *J Environ Manag*, 74 (2005) 207.
78 Cheng J, *ACS Omega*, 5 (2020) 5389.
79 Surip S, *Surf Interfaces*, 21 (2020) 100641.
80 Liu X J, Li M F & Singh S K, *J Mater Res Technol*, 12 (2021) 1434.
81 Mittal H, *J Polym Environ*, 28 (2020) 1637.